

Hydro-Mechanics Analysis on the Strength Development of Cement-Stabilized Sand

Fangtong WANG^a, Dianqing LI^a and Yong LIU^{a,1}

^a*State Key Laboratory of Water Resources and Hydropower Engineering Science, Institute of Engineering Risk and Disaster Prevention, Wuhan University, Wuhan, Hubei, China*

Abstract. Deep cement mixing is an effective ground stabilization technique to control the ground movement on sand areas, and most of the projects have the problem of seepage. The cement slurry is in a fluid state before the initial setting time, the seepage may affect the diffusion process of cement slurry during this period. A hydro-mechanical approach is proposed to investigate the interaction between the seepage and the strength of cement-stabilized sand. The diffusion of the cement slurry under seepage is considered in this study and the diffusion process is simulated by the finite element method. According to the cement concentration at the end of the diffusion process, the strength of cement-stabilized sand can be predicted by combining an empirical formula. Simulation results examine that the existence of seepage and cracks can enhance the non-uniform diffusion process of cement slurry, and the actual strength distribution of the deep cement-mixed sand is far from the ideal state. This indicates that the influence of seepage on the strength of cement-stabilized sand should be considered in the design of projects.

Keywords. Deep soil mixing, seepage, cement-stabilized soil, FEM analysis

1. Introduction

Saturated sand often has a low strength value and is prone to liquefaction during an earthquake. As a result, the safety and durability of the structures constructed on sandy areas may be adversely influenced due to the characteristics of saturated sand. In addition, seepage often exists in the areas of saturated sand. Especially, the permeability of sand is generally larger than other types of soil (such as clay and silt) [1,2], which further intensifies the seepage process. Deep soil mixing (DSM) is a widely used ground improvement and seepage control technique, which can be used for sandy areas as the pile foundation or cut-off wall [3]. However, the cement-sand mixture is flowable before the initial setting time of cement. The seepage can carry away the cement slurry and change the shape and strength distribution of a DSM pile. However, few previous studies on grouting considered the condition of seepage. In recent years, grouting under seepage has drawn more attention. Several theoretical and numerical models have been proposed to calculate grout penetration by considering the seepage speed [4,5]. Gurspersaud et al. [6] conducted an in-situ test of grouting under

¹ Yong Liu, State Key Laboratory of Water Resources and Hydropower Engineering Science, Institute of Engineering Risk and Disaster Prevention, Wuhan University, Wuhan, Hubei, China; E-mail: liuy203@whu.edu.cn.

the condition of existing seepage. Liu et al. [7] conducted a series of physical simulation experiments to investigate the effects of nanoparticles on the grouting performance in dynamic water conditions. Most of these investigations were focused on the grouting experimental research in fractured rock, few studies investigated the case of DSM pile. To fill this gap, a case study of DSM pile is conducted in this study, where the time-dependent characteristic of cement slurry and the variation of permeability and strength with depth are also considered. The shape and the contours of seepage velocity and strength of the DSM pile are presented. The simulation results may provide the reference for the related projects.

2. Numerical Model

The case study that the concentration diffusion of deep soil mixing pile affected by dynamic water before the initial setting time was conducted in this study. The size and boundary conditions of the finite element model are shown in figure 1. The material of the surrounding soil is sand, and thus, the material of the DSM pile is a cement-sand mixture. The diameter and length of the DSM pile are 0.6 m and 20 m, respectively. On the left side of the model exists a static water pressure p_w , it can be calculated by:

$$p_w = \rho_w gh \quad (1)$$

where ρ_w is the density of water; g is the gravitational acceleration; h is the depth. Two surfaces parallel to the direction of water pressure are undrained boundaries. The right side of the model is a drained boundary, and the p_w is constant 0.

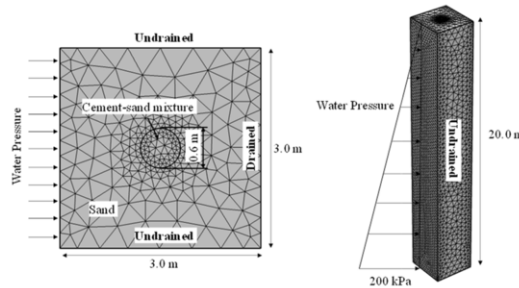


Figure 1. Schematic diagram of finite element model size and boundary conditions.

Two-phase Darcy's law was used herein to describe the diffusion and flow state of cement slurry under the condition of seepage. The water and slurry are both considered Newtonian fluid and incompressible. The porous media (sand) is considered isotropic. The continuity equation of two-phase Darcy's law can be written as:

$$-\left[\frac{\partial(\rho_c v_{cx})}{\partial x} + \frac{\partial(\rho_c v_{cy})}{\partial y} + \frac{\partial(\rho_c v_{cz})}{\partial z} \right] = \frac{\partial(\rho_c n S_c)}{\partial t} \quad (2)$$

$$-\left[\frac{\partial(\rho_w v_{wx})}{\partial x} + \frac{\partial(\rho_w v_{wy})}{\partial y} + \frac{\partial(\rho_w v_{wz})}{\partial z}\right] = \frac{\partial(\rho_w n S_w)}{\partial t} \quad (3)$$

$$S_c + S_w = 1 \quad (4)$$

where ρ_c is the density of cement-sand mixture; v_{cx} , v_{cy} , and v_{cz} are the seepage velocity of cement slurry in x , y , z directions; v_{wx} , v_{wy} , and v_{wz} are the seepage velocity of water in x , y , z directions; S_c and S_w are the volume fraction of cement-sand mixture and water, respectively; n is the porosity of sand.

The porosity is related to the vertical soil pressure p_s . The p_s can be calculated by:

$$p_s = \rho_{sat} g h \quad (5)$$

where ρ_{sat} is the saturated density of sand.

According to the compressibility characteristic of soil, n can be expressed as:

$$n = \frac{e}{1+e} = \frac{\Gamma - C_c \lg p_s}{1 + (\Gamma - C_c \lg p_s)} \quad (6)$$

where e is the void ratio; C_c is the compression index of sand; Γ is the intercept of the e - $\log p$ curve.

The seepage velocity v can be calculated by:

$$v = \frac{k \rho g}{\mu} i = k (S_c \rho_c + S_w \rho_w) \left(\frac{S_c}{\mu_c} + \frac{S_w}{\mu_w} \right) g i \quad (7)$$

where k is the permeability of sand; ρ is the density of fluid; μ is the coefficient of dynamic viscosity of fluid; i is the hydraulic gradient; μ_c and μ_w are the coefficient of dynamic viscosity of the cement-sand mixture.

According to the empirical formula proposed by Samarasinghe et al. [8], The permeability k also can be calculated by:

$$k = K \frac{\mu_w}{\rho_w g} = C \frac{e^m \mu_w}{(1+e) \rho_w g} \quad (8)$$

where C and m are fitting parameters.

Combining with Eqs. (5), (6), and (8), the variation of k with h can be calculated. In addition, considering the time-dependent characteristic of μ_c , it can be expressed as:

$$\mu_c = \mu_{c,0} e^{Bt} \quad (9)$$

where $\mu_{c,0}$ is the initial coefficient of dynamic viscosity of slurry; B is the fitting parameter.

The strength of cement-stabilized sand is affected by the cement mark, cement content, and water-cement ratio of the mixture. The non-linear relationship between S_c and these parameters is not considered herein for simplicity. Thus, a linear relationship between the strength and S_c is built for as follows:

$$q_u = (q_{\max} - q_s) S_c + q_s \quad (10)$$

where q_u is the strength of cement-stabilized sand, q_{\max} is the strength of cement-stabilized sand when $S_c = 1$; q_s is the strength of sand. The q_s in various depths also can be calculated based on the Mohr-Coulomb criterion. According to the test data of [9,10], the material parameters are summarized in table 1.

Table 1. Summary of material parameters.

Parameter	Value	Unit	Parameter	Value	Unit
Saturated density of sand, ρ_{sat}	1800	kg/m ³	Cement content, A_w	10	%
Density of cement-sand mixture, ρ_c	1600	kg/m ³	Strength of cement-stabilized sand when $S_c = 1$, q_{\max}	2100	kPa
Density of water, ρ_w	1000	kg/m ³	Cohesive force, c	0	kPa
Compression index of sand, C_c	0.14	kPa ⁻¹	Internal friction angle, ϕ	30	°
Intercept of the e -log p curve, Γ	1.13	1	Fitting parameter, B	0.022	s ⁻¹
Coefficient of dynamic viscosity of water, μ_w	0.899	mPa·s	Fitting parameter, C	0.16	m/s
Initial coefficient of dynamic viscosity of cement-sand mixture, $\mu_{c,0}$	7.204	mPa·s	Fitting parameter, m	7.5	1
Minimum water-cement ratio, w/c_{\min}	1	1			

3. Results and Discussion

S_c and v at different times are analyzed in this study. Several cross-sections were selected to visually describe the numerical results. The contours of S_c and are the seepage velocity v shown in figure 2. It can be found that the volume fraction of the cement-sand mixture changes with time, and the slurry significantly diffuses along the direction of seepage. In addition, the cross-sectional shape of the DSM pile also becomes irregular, and the degree of irregularity increases with time and depth. Although the k is high near the surface, the effect of seepage is not obvious due to the small hydraulic gradient. In addition, the seepage velocity increases with depth. It means the effect of the variation of the hydraulic gradient with depth on seepage velocity is greater than that of permeability in this case. In addition, the cement-sand mixture can affect the direction and magnitude of seepage velocity. The seepage velocity of slurry is lower than that of water due to the high coefficient of dynamic

viscosity. Because of the obstruction of slurry, the seepage velocity of the left and right sides of the slurry is lower than the surrounding area. Under the influence of seepage, the cross-sectional shape of the DSM pile changes from a regular circle to an irregular cone. It causes a larger seepage velocity of the upper and lower sides of the slurry.

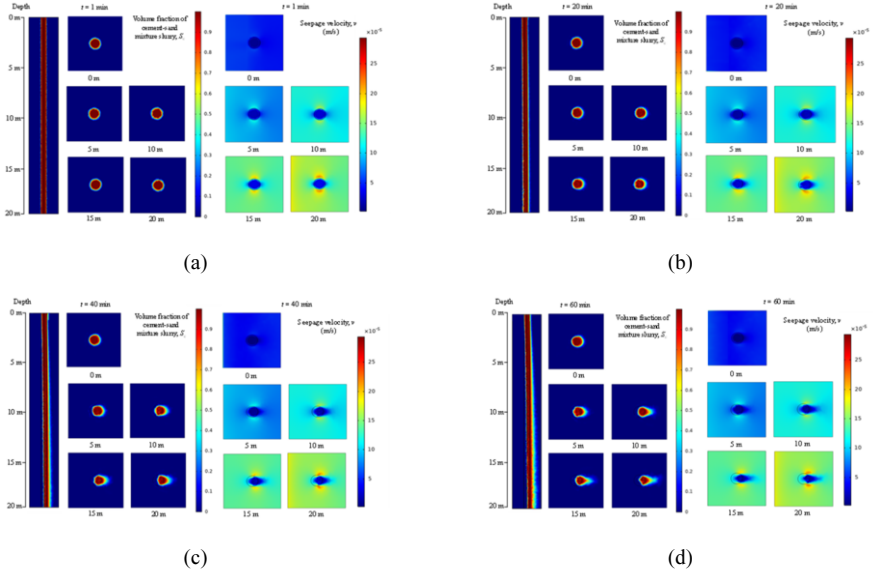


Figure 2. Contours of S_c and v in different depths when (a) $t=1$ min; (b) $t=20$ min; (c) $t=40$ min; (d) $t=60$ min.

According to the simulation results, seepage may cause the DSM pile to tilt, and the inclined angle θ of the DSM pile at different times is shown in figure 3. The trend of the θ - t curve is nonlinear, and the growth rate gradually decreases over time. It is due to the time-dependent characteristic of μ_c . The inclined angle increases with time, and the maximum value is 0.95° at 60 min. The corresponding deviation value of the bottom of the pile ε can be calculated by:

$$\varepsilon = \frac{L \tan \theta}{D} \times 100\% \quad (11)$$

where L and D are the length and the diameter of the pile, respectively. The L and D are 20 m and 0.6 m herein. Thus, ε is 55% in this study. This far exceeds the allowable deviation value of 1%. It indicates that the construction quality is not the only factor that can cause pile tilt, strong seepage can also lead to this problem. In addition, because the effect of seepage is not obvious near the surface, it is difficult to accurately control the quality of the DSM pile in areas where seepage exists in actual projects.

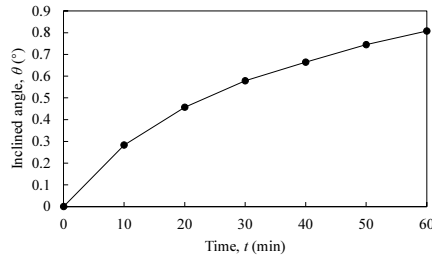


Figure 3. Inclined angle of DSM pile at different times.

Five cutting lines were set herein to show the influence of the seepage on the strength of different locations. The strength q_u can be calculated by the simulation results of S_c and Eq. (10). The locations of these five cutting lines are shown in figure 4(a), and the strength changes with depth and time on cutting lines 1 to 5 are shown in figures 4(b) to (f), respectively. The strength at 17 m on cutting line 1 decreases obviously at 40 min, and the strength at 18 m is the same as the surrounding soil at 60 min. It indicates that the deviation of the bottom of the pile larger than 50% at 60 min because of the seepage. The location of cutting lines 2 and 4 are symmetrical. The distribution of strength along depth is similar at 1 min. However, under the condition of seepage, the strength on cutting lines 2 gradually decreases, and finally the cement slurry was completely carried away, the strength decreases to q_s . Meanwhile, the cement slurry was carried to the right side. The strength on cutting line 4 increases with time, and finally to the value of q_{max} . The trend of strength on cutting lines 3 and 5 over time is like that of cutting lines 2 and 4. The difference is that the slurry cannot reach the location of cutting line 3, and the strength on cut 5 also cannot reach the q_{max} due to the great distance from cutting line 1. Based on the simulation results, the effect of seepage on the diffusion of cement slurry cannot be neglected in sand areas. The water-cement ratio, cement content, and construction method should be optimized to reduce the influence of seepage on construction quality.

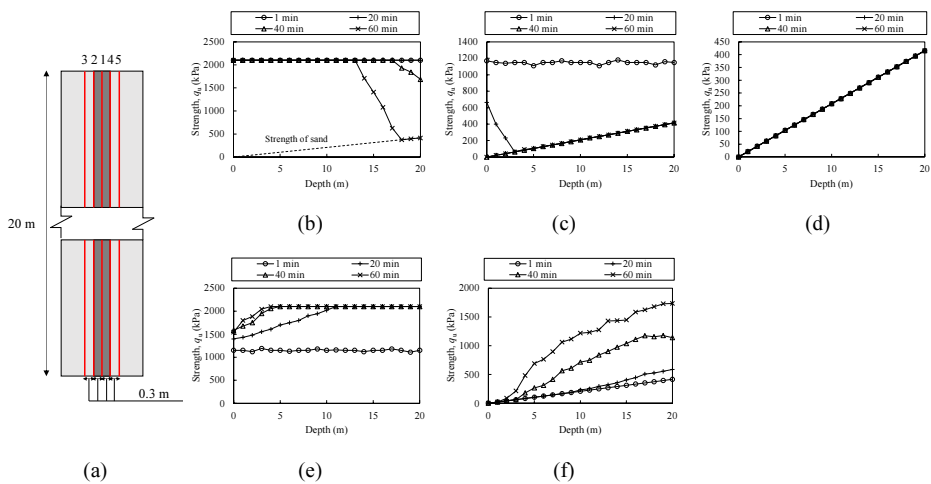


Figure 4. (a) Locations of five cutting lines and the strength change with depth and time on cutting line (b) 1; (c) 2; (d) 3; (e) 4; (f) 5.

4. Conclusion

A finite element analysis was conducted to study the influence of seepage on DSM pile. The simulation results indicate that the cement slurry will diffuse along the direction of seepage. The degree of influence increases with the increase of depth, and the contours of seepage velocity can prove it. The seepage velocity increases with depth, and with the change of the shape of the pile's cross-section. The seepage velocity at the upper and lower sides of the DSM pile will increase and larger than the seepage velocity of the surrounding soil. The seepage can cause the DSM pile to tilt due to the cement slurry is carried away. S_c of the left side of the DSM pile decreases over time, and meanwhile, S_c of the right-side increases. The vertical deviation of the pile is much greater than the permissible value due to the seepage. Especially, the strength of the DSM pile is affected directly by the distribution of S_c . Thus, the seepage problem needs to be emphasized in actual projects.

Acknowledgments

This research is supported by the National Natural Science foundation of China (Grant No.: 51879203) and the NRF-NSFC 3rd Joint Research Grant (Earth Science) (Grant No.: 41861144022).

Competing interests

The authors have declared that no competing interests exist.

References

- [1] Wang F, Li D, Du W, Zarei C, Liu Y. Bender element measurement for small-strain shear modulus of compacted loess. *International Journal of Geomechanics*. 2021 May; 21(5): 04021063.
- [2] Chen G, Wang FT, Li DQ, Liu Y. Dyadic wavelet analysis of bender element signals in determining shear wave velocity. *Canadian Geotechnical Journal*. 2020 March; 57(12): 2027-2030.
- [3] Liu Y, Jiang YJ, Xiao H, Lee FH. Determination of representative strength of deep cement-mixed clay from core strength data. *Géotechnique*. 2017 April; 67(4): 350-364.
- [4] Tani ME. Grouting rock fractures with cement grout. *Rock Mechanics and Rock Engineering*. 2012 March; 45(4): 547-561.
- [5] Watson C, Wilson J, Savage D, Benbow S, Norris S. Modelling reactions between alkaline fluids and fractured rock: The Maqarin natural analogue. *Applied Clay Science*. 2016 March; 121: 46-56.
- [6] Gurbarsad N, Lees D, Hu F. Jet grouting for seepage control at Lac Des Iles (LDI) water management facility. In Suleiman MT, Lemnitzer A, Stuedlein AW, IFCEE 2018: Case Histories and Lessons Learned; 2018 March 5-10; Orlando, Florida: ASCE; 2018. p. 139-149.
- [7] Liu YH, Yang P, Ku T, Gao SW. Effect of different nanoparticles on the grouting performance of cement-based grouts in dynamic water condition. *Construction and Building Materials*. 2020 July; 248: 118663.
- [8] Samarasinghe AM, Huang YH, Drnevich VP. Permeability and consolidation of normally consolidated soils. *Journal of the Geotechnical Engineering Division*. 1982 June; 108(6): 835-850.
- [9] Qian K, Wang X, Chen J, Liu P. Experimental study on permeability of calcareous sand for islands in the South China Sea. *Rock and Soil Mechanics*. 2017 June; 38(6): 1557-1564.
- [10] Sha F, Li S, Lin C, Liu R, Zhang Q, Lei Y, Li Z. Research on penetration grouting diffusion experiment and reinforcement mechanism for sandy soil porous media. *Rock and Soil Mechanics*. 2019 November; 40(11): 4260-4269.